Indian Journal of Chemistry
Vol. 61, January 2022, pp. 21-30

Synthesis of photoactivable Pt(IV) prodrug loaded on $NaYF_4$ based upconversion nanoparticles functionalized with 2-deoxy-D-glucose and its evaluation for targeted cancer therapy

K Shitaljit Sharma[a,b], Lodestarborn Tiewsoh[c], Akhil K Dubey[d], Prasad P Phadnis[a,e,*], V Sudarsan[a,e] & Rajesh K Vatsa[e,f,*]

[a]Chemistry Division, Bhabha Atomic Research Centre, Trombay, Mumbai 400 085, India
[b]Department of Chemistry, Mizoram University, Aizawl 796 009, India
[c]North-Eastern Hill University, Shillong 793 022, India
[d]Bio-Organic Division, Bhabha Atomic Research Centre, Mumbai 400 085, India
[e]Homi Bhabha National Institute, Anushaktinagar, Mumbai 400 094, India
[f]Department of Atomic Energy, Mumbai 400 001, India

*E-mail: phadnisp@barc.gov.in (PPP)/ rajesh.vatsa@dae.gov.in (RKV)

Received 21 October 2021; revised and accepted 08 December 2021

Nano-formulation based on Tm, Yb doped $NaYF_4$ upconversion nanoparticles (UCNPs) functionalized with 2-deoxy-D-glucose have been synthesized to load the photoactivable Pt(IV) prodrug, cis-$[PtI_2(NH_3)_2(OCOCH_2CH_2COOH)_2]$. The Pt(IV) prodrug has been synthesized by oxidation of cis-$[PtI_2(NH_3)_2]$ to $[PtI_2(OH)_2(NH_3)_2]$ and its further treatment with succinic anhydride. It is loaded through ester bond formation between the carboxyl groups of Pt(IV) prodrug with hydroxyl groups of 2-deoxy-D-glucose (2-DG) coated on UCNPs. The cytotoxicity of formulation after exposing to 385 nm UV light and in absence of light is evaluated against MCF-7 cell lines by MTT assay. The results have revealed enhanced cytotoxicity of UV exposed nano-formulation. Additionally, the clonogenic assay has exhibited the decrease in plating efficiency as inferred from decreased surviving fraction around 20% only for UV activated formulation as compared to formulation in dark, as well as merely Pt(IV) prodrug. These results are indicative that more internalization of the formulation inside the cancer cells was achieved due to the presence of 2-DG rendering more efficiency to kill cancer cells.

Keywords: Photoactivable, Pt(IV) prodrug, Upconversion nanoparticles, 2-deoxy-D-glucose, Internalization, Clonogenic assay

Cisplatin and its analogues are widely used for the treatment of nearly 70% of cancers ranging from ovarian, head and neck, bladder, cervical to lymphoma cancers[1] by interacting with DNA and forming interstrand cross-link between N-7 atoms of two adjacent guanine (G) residues and Pt(II) center[2]. They also interact with many other biomolecules containing methionine and cysteine residues[3] causing severe side-effects like nephrotoxicity, ototoxicity, neurotoxicity, haematological toxicity and seizures. Among these, nephrotoxicity is the serious issue[4]. Out of many strategies that have been employed to overcome these issues, the strategies based on Pt(IV) prodrug which can be activated by physiological characteristics of tumours or by light, have special advantages[5,6]. The Pt(IV) prodrugs which can be activated by light are usually found to be non-toxic in absence of light exposure but cause toxicity to the desired regions when exposed to an external light of wavelength typically lying between 315-500 nm[7]. Usually, the exciting light does not have deep penetration through thick mass of body for activating Pt(IV) prodrug accumulated inside deeper organs[8,9]. To overcome this limitation, the use of upconversion nanoparticles (UCNPs) based nano-formulation that act as host as well as activator is a main focus for the present day research[10]. Upconversion is an anti-Stokes shifted phenomenon associated with the absorption of two or more photon of a deep penetrating light and its emission at the shorter wavelength[11]. Among UCNPs, hexagonal $NaYF_4$ based UCNPs have been widely studied because of their high quantum yields[12]. Many $NaYF_4$ based nano-formulations tagged with targeting groups like folic acid or peptide have been prepared and studied for drug delivery, drug activation including photodynamic therapy as well as diagnosis[13]. The major challenge for the use of nano-formulations is their inability to cross reticuloendothelial system (RES) which is mostly governed by the surface charge of the nano-

formulations. It has been reported that the nano-formulations bearing negative charge or neutral have more tendency to cross RES[14]. The problem with negatively charged nano-formulation is the difficulty for their cellular internalization due to the similarity in charge with the cell membrane even though it reaches at the targeted site. Additionally, for nano-formulations having the neutral surface charge, choice of proper functional groups is a major challenge. Among neutral nano-formulations, hydroxyl group functionalized nano-formulations have been reported to exhibit high blood retention time. As a result, many nano-formulations based on dextran have been studied but later on, they were found to be unstable due to hydrolysis of bonds at the binding sites[15].

Considering these facts, photoactivable Pt(IV) prodrug of a cisplatin derivative has been synthesized, loaded on nano-formulation based on hexagonal $NaYF_4$ doped with Yb (18%) and Tm (2%) which has nearly neutral surface charge due to the presence of a 2-deoxy-D-glucose (2-DG) derivative on the surface and studied with MCF-7 cell lines with the main focus on delivery of photoactivable Pt(IV) prodrug and their activation to cisplatin using the light activated UCNPs. Generally, cancer cells have huge demand for D-glucose for their metabolic activities in order to supplement nutrients and energy required for their rapid proliferation through glycolysis pathway[16]. Whereas administration of 2-deoxy-D-glucose which mimic D-glucose and lack hydroxyl groups at C-2 position, leads to inhibition of glycolysis by avoiding the conversion of glucose-6-phosphate to fructose-6-phosphate[17]. Besides the inhibition of glycolysis, the presence of 2-DG on the surface of nano-formulation not only directs to target the tumor site but also provides the site for loading Pt(IV) prodrug by forming an ester bond. In our earlier work, we have successfully shown faster uptake of 2-DG coated UCNPs, their cytotoxicity and their ability for bio-imaging. It was very clear that the cytotoxic application of 2-DG coated UCNPs formulation was governed by 2-DG strategy[18]. In view of this and in continuation of our work, we have developed and evaluated the photoactivated Pt(IV) prodrug loaded UCNPs formulation against MCF-7 human breast cancer cell lines. Our initial interesting results have been reported herein.

Experimental Details

Paraformaldehyde, 2-deoxy-D-glucose, yttrium acetate, thulium acetate, ytterbium acetate, oleic acid, 1-octadecene, sodium hydroxide, ammonium hydrogen fluoride, Igepal CO-520, (3-aminopropyl) trimethoxysilane (APTMS), tetraethyl orthosilicate (TEOS), HBr (33%) in acetic acid, pyridine, zinc metal, ammonium chloride, Dowex-500 resin, lithium bromide, potassium bromide and tetra-n-butylammonium bromide (TBAB), N,N′-dicyclohexylcarbodiimide (DCC), 4-dimethylaminopyridine (DMAP), benzoyl chloride, acetic acid, were purchased from Sigma Chemical Company (St Louis, MO, USA). Hoechst 33342 was purchased from Molecular Probes Life Technologies (Eugene, OR, USA). Trypsin-EDTA, foetal bovine serum, antibiotic solution and Dulbecco's Modified Eagle's medium (DMEM) were purchased from Himedia Laboratories (Mumbai, India). Acetic anhydride was purchased from Spectrochem (Mumbai, India). All the chemicals used in these studies were of analytical grade. All the solvents were dried by following the standard protocol[19].

The Pt(IV) prodrug was purified by recrystallization in ethanol-water mixture at room temperature. The NMR spectral analyses were performed on the Agilent/ Varian 600 MHz NMR spectrometer with a Unity Inova console operating at 599.88 (^{1}H) and 150.84 (^{13}C{^{1}H}). The ^{1}H and ^{13}C{^{1}H} NMR chemical shifts were relative to internal $CHCl_3$ or DMSO peaks in case of $CDCl_3$ or DMSO-d_6 solutions, respectively. The UCNPs sample was authenticated by powder X-ray diffraction (XRD), transmission electron microscopy (TEM), Fourier transform infrared spectroscopy (FT-IR), zeta-potential studies and photoluminescence studies. The sample for studying the XRD was prepared by dispersing the sample in a minimum amount of cyclohexane and pouring drop by drop to the sample holder and for the silica coated sample, the sample was dispersed in a minimum amount of methanol and followed the same procedure. The XRD pattern of the samples were recorded on a Phillips Model PW1710 diffractometer with Cu-Kα (λ = 1.545 Å) radiation. For TEM imaging, a drop of dilute dispersed solution of test sample in hexane or methanol was poured on the carbon coated copper-grid of 200 mesh size and dried under an IR lamp for 30 min. A transmission electron micrograph was obtained using a Philips CM 200 TEM system for particle size determination. The zeta-potential measurements were performed using Zetasizer nano series (Malvern Instruments). The infrared spectra were recorded in the range of

400-4000 cm^{-1} on a Fourier transform infrared (FT-IR) spectrometer (Women Hartman and Braun, MB 100 series). The photoluminescence studies were carried with the help of Edinburgh Instrument FLS920 equipped with a 450 W xenon arc lamp having Peltier element cooled red sensitive Hamamatsu R955 PMT. The sample was dispersed in hexane or methanol, placed in a cuvette or as a solid layer on glass slide and emission spectrum was recorded upon 980 nm laser excitation.

Synthesis of $NaYF_4$ doped with Tm and Yb[20]

Yttrium acetate (1.0 g, 3.75 mmol), thulium acetate (64.8 mg, 0.18 mmol) and ytterbium acetate (263 mg, 0.75 mmol) were dissolved in the mixture of oleic acid (5 mL) and 1-octadecene (30 mL) contained in a three-necked round bottom flask. Sodium hydroxide (600 mg, 15 mmol) and ammonium hydrogen fluoride (555 mg, 15 mmol) dissolved in methanol were added and heated up to 100 °C under an inert atmosphere of argon. After evaporating the methanol layer resulting in formation of yellow liquid, the reaction mixture was heated till 300 °C with the heating rate of 5 °C per min. The reaction mixture was heated further at the same temperature for 2 h and then cooled to the room temperature. The nanoparticles were precipitated by addition of acetone, dispersed in a minimum amount of hexane and precipitated with acetone. The process was repeated three times. The obtained nanoparticles were characterized as $NaYF_4$ by X-ray diffraction (XRD), transmission electron microscopy (TEM) and photoluminescence studies.

Synthesis of silica coated upconversion nanoparticles ($NaYF_4$: Tm and Yb)[21]

To a conical flask (50 mL) containing 20 mL of cyclohexane, Igepal CO-520 (0.5 g) was added, stirred for 15 min. A dispersion solution of UCNPs (10 mL; 1 mg/2 mL of cyclohexane *i.e.,* 5 mg) was added and stirred for 20 min which was followed by the addition of ammonia solution (500 µL). After stirring for additional 20 min, TEOS (200 µL) was added with an interval of 12 h to 48 h. The APTMS (200 µL) was added and stirred for additional 24 h. Methanol (10 mL) was added and separation of the phase between cyclohexane and methanol layers was done. The particles were collected from methanol layer by the centrifugation. The particles were characterized with TEM and FT-IR analyses.

Synthesis of isothiocyanate derivative of 2-deoxy-D-glucose

An isothiocyanate derivative of 2-DG was prepared according to the Scheme 1 and was characterized by NMR spectroscopy (Supplementary Data, Fig. S1-S9). The obtained 2-deoxy-*O*-glucose isothiocyante was further used to functionalize the amine functionalized UCNPs.

Functionalization of amine functionalized UCNPs with 2-DG

To a 3,4,5-tri-*O*-benzoyl-2-deoxyglycopyranosyl isothiocyanate (150 mg) dissolved at DMF (5 mL), amine functionalized UCNPs were added and heated at 60 °C for 8 h. The nanoparticles were collected by centrifugation and washed with acetone three times. The nanoparticles were dispersed in the ammonia solution (33%, 15 mL) and stirred for 10-12 h at room temperature. The nanoparticles were collected by centrifugation, washed with water followed by acetone and characterized by FT-IR spectroscopy and elemental analysis. The reaction is shown in Scheme 2.

Synthesis of Pt(IV) prodrug of cisplatin derivative[22]

The synthesis of this Pt(IV) prodrug was performed with the slight modifications in the literature

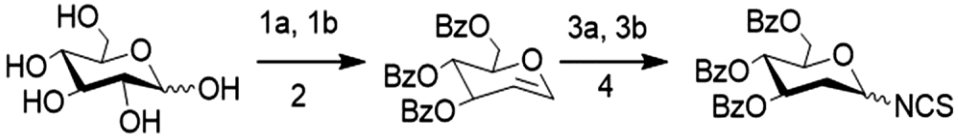

Scheme 1 — (1a) benzoyl chloride, pyridine; (1b) HBr (33%) in acetic acid, DCM; (2) Zn, NH_4Cl in acetonitrile, reflux; (3a) Dowex-500 resin, LiBr, H_2O; Ac_2O, pyridine; (3b) HBr (33%) in acetic acid, DCM; (4) KSCN, TBAB, reflux

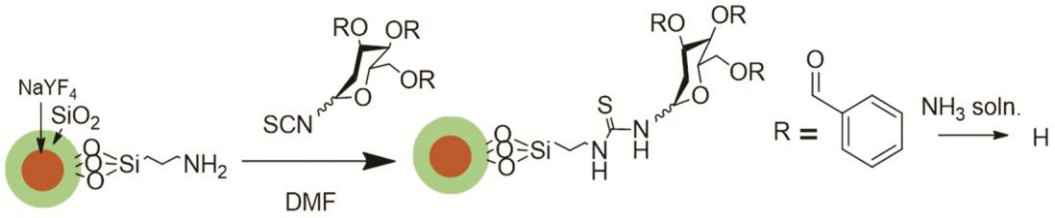

Scheme 2 — Functionalization of amine functionalized UCNPs with 2-DG

procedure. Briefly, to K_2PtCl_4 (100 mg, 0.25 mmol) solution in water (10 mL), a saturated aqueous solution of KI was added till the colour of the solution appeared as dark brown. After stirring for 15 min, ammonium chloride (26.75 mg, 0.5 mmol) was added and the pH of the reaction mixture was adjusted to 12 by slow addition of 1 mM NaOH solution. The precipitate formed was filtered out, washed with water and treated with H_2O_2 solution. The reaction mixture was wrapped with aluminium foil to protect from light. The reaction mixture was concentrated using a rotavapour placed in a dark room and a dark brown solid was obtained. The solid was dissolved in dry DMSO (2 mL) and treated with succinic anhydride (40 mg, 0.4 mmol). The compound obtained was washed with dried acetone and dried under reduced pressure. The entire reaction (Scheme 3) was performed under subdued light conditions. The compound was characterized with NMR (^{1}H & ^{13}C{^{1}H}) spectroscopy.

Loading of Pt(IV) prodrug on 2-DG coated UCNPs[23]

The loading of the Pt(IV) prodrug was done by forming ester bond between the carboxyl functional group of Pt(IV) prodrug and the hydroxyl groups of 2-DG coated UCNPs using DCC as coupling agent in a dry DMF as shown in Scheme 4. To a solution of Pt(IV) prodrug (0.1 mmol) in DMF (5 mL), DCC (0.12 mmol) was added at 0 °C and stirred for 3 h at room temperature. To the above solution, UCNPs (30 mg) dispersed in DMF (5 mL) and a catalytic amount of 4-dimethylaminopyridine (DMAP) were added and stirred for 10-12 h. Then the UCNPs were collected by centrifugation and the unbound prodrug was removed by the dialysis using saline solution (0.9 M) as the medium. The amount of Pt(IV) prodrug loaded on UCNPs was quantified using ICP-OES. The obtained nanoparticles are henceforth referred as UCNPs-Pt(IV) for simplicity.

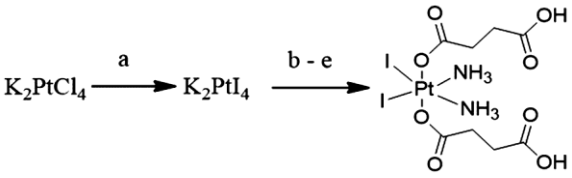

Scheme 3 — Synthesis of Pt(IV) prodrug of cisplatin derivatives by reacting K_2PtCl_4 with (a) KI, (b) NH_4Cl, (c) NaOH, (d) H_2O_2 and (e) succinic anhydride

Cell culture experiments

MCF-7 cells were procured from American Type Culture Collection (ATCC) and maintained as monolayer using DMEM media supplemented with 10% fetal bovine serum at 37 °C with 5% CO_2 in a humidified environment. For every experiment, seeding of cells was done one day prior to the experiment. After treating the cells with the nano-formulations and corresponding drugs, cells were exposed to 385 nm UV light or 980 nm laser. Cell survival studies were conducted by MTT assay. For 980 nm exposure experiment, cells were seeded in separate 96 well plates. In case of clonogenic assay, treated cells and control cells were only exposed with 395 nm UV light.

Cytotoxicity study by MTT assay[24]

MTT assay was performed in accordance with the standard protocol. Briefly, to a 96 well plate, MCF-7 cells (5000 to 15000 cells per well) were seeded and treated with 2-DG functionalized UCNPs with concentration ranging from 100 – 1000 µg/mL for a time period ranging from 24 h to 72 h. Then the MTT solution (50 µl; stock solution = 5 mg/mL) was added followed by incubation of test samples. After incubating for 3 h, DMSO (150 µL) was added in each well, mixed using a pipette to fully dissolve the

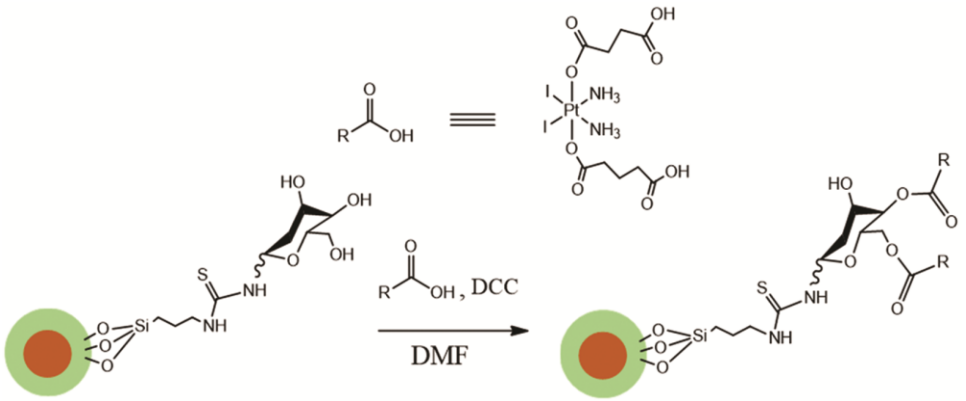

Scheme 4 — Loading of Pt(IV) prodrug on 2-deoxy-D-glucose coated UCNPs

formazan formed after addition of MTT reagent. The absorbance (A) was measured at 590 nm using a plate reader.

The percentage of the cell survival was calculated by dividing the absorbance reading of the sample obtained after subtracting the values of the blank by the values of the control obtained after subtracting the values of blank and followed by multiplication by 100 as shown in Eqn. (1).

$$\% \text{ of cell survival} = \frac{A_{Sample} - A_{Blank}}{A_{Control} - A_{Blank}} \times 100 \quad \ldots (1)$$

Clonogenic assay[25,26]

To a 6 well plate, MCF-7 cells (500 per well) were seeded and treated with increasing concentrations of Pt(IV) prodrug and UCNPs-Pt(IV) (5 µL, 10 µL and 20 µL). The cells were allowed to form colonies. As the required size of colonies for control was attained, the cell culture media were removed and washed with phosphate buffered saline (PBS). For fixing, the cells were incubated at 4 °C for 2 h after treating with formaldehyde (6 %). The cells were stained with 0.5% crystal violet. The excess dye was washed out with water. The number of colonies formed per well were counted and analyzed according to the standard protocol.

Plating efficiency (PE) was evaluated. The PE is the ratio of the number of colonies to the number of cells seeded as shown below in Eqn. (2).

$$PE = \frac{\text{No.of colonies formed}}{\text{No.of cells seeded}} \times 100 \quad \ldots (2)$$

The number of colonies that arise after treatment of cells, which are expressed in terms of PE, is called the surviving fraction (SF) (Eqn. (3)).

$$SF = \frac{\text{No.of colonies formed after treatment}}{\text{No.of cells seeded} \times PE} \times 100 \quad \ldots (3)$$

Results and Discussion

The synthesis of the non-agglomerated nanoparticles is desired for biological applications. The use of fatty acids during the synthesis of the nanoparticles has been reported for avoiding the agglomeration. The fatty acids help to avoid the agglomeration by inhibiting the interactions of nanoparticles. So, the synthesis of UCNPs based on $NaYF_4$ doped with Tm (2%) and Yb (18%) was done by thermolysis method using oleic acid as the capping agent and 1-octadecene as the solvent upon heating at 320 °C by minor modifications in literature methods[27,28]. The synthesized UCNPs were found to be dispersible in non-polar solvent like cyclohexane and chloroform and they were white semi-solid in nature. The formation of the standard hexagonal phase β-$NaYF_4$:Yb (18%), Tm (2%) was confirmed by comparing with the standard XRD pattern (JCPDS: 28-1192). The broad peak at 20° in XRD pattern (Fig. 1a) represents the amorphous nature due to the organic content *i.e.*, oleic acid. The presence of the oleic acid on the surface of the UCNPs made the nanoparticles to be dispersible in non-polar solvent like hexane, chloroform and toluene *etc.* The XRD pattern of $NaYF_4$@SiO_2 is shown in Fig. 1b. The presence of the broad peak centred at around $2\theta = 20°$ corresponds to the amorphous silica which also confirmed the formation of silica layer on the surface of $NaYF_4$.

The morphological studies of the synthesized UCNPs were done by TEM. The shape of the UCNPs was observed to be cuboid with the average size in the range of 24±1 nm (Fig. 2a) and no agglomeration of the UCNPs was observed. The particle distribution is shown in Fig. 2b. When the selected area electron diffraction (SAED) pattern was taken for the synthesized UCNPs (Fig. 2c), the diffraction pattern

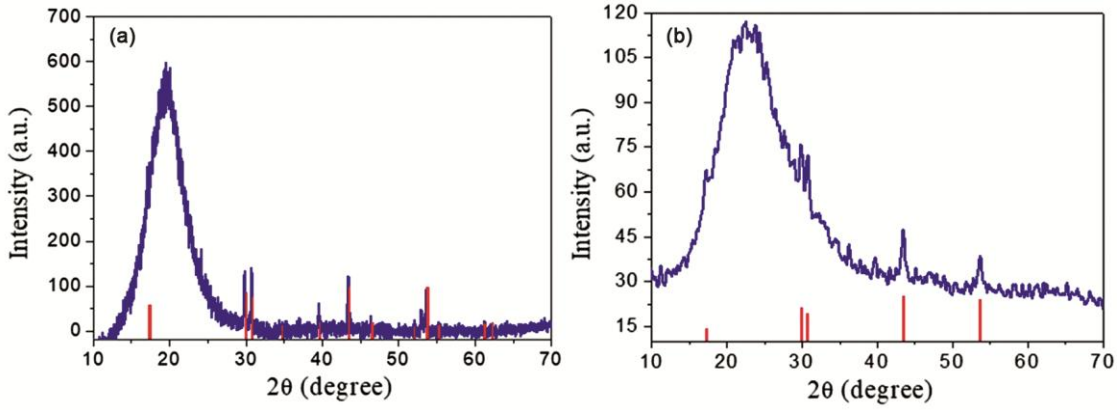

Fig. 1 — X-diffractograms of (a) $NaYF_4$:Tm,Yb and (b) $NaYF_4$:Tm,Yb@SiO_2 UCNPs

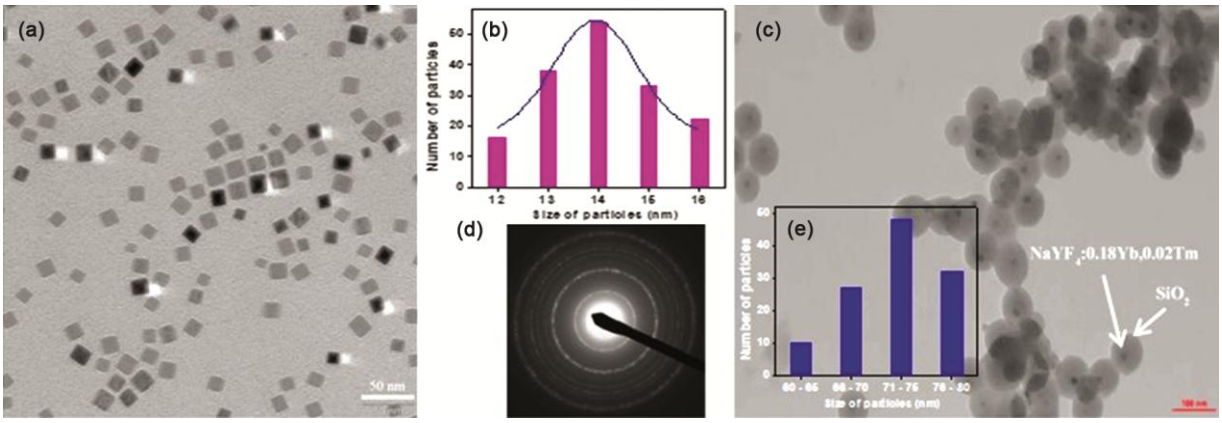

Fig. 2 — Characterization of (a) $NaYF_4$:0.18Yb,0.02Tm by TEM with corresponding (b) particle distribution and (c) SAED pattern; (d) TEM of $NaYF_4$:0.18Yb,0.02Tm@SiO_2 with (e) particle distribution

with ring fringes was observed. This further confirms that the synthesized UCNPs were crystalline[18].

For the biological applications, the synthesized nanoparticles should be dispersible in water. But, the presence of oleic acid on the surface of the nanoparticles, made UCNPs to be dispersible in the nonpolar solvent like chloroform or hexane. To convert the hydrophobic nature to the hydrophilic, the nanoparticles were coated with silica[27,28] avoiding the agglomeration using tetraethyl orthosilicate (TEOS) and Igepal CO-520 as the surfactant. The hydrocarbon chain of the Igepal CO-520 interacts with the hydrophobic part of the oleic acid. But the hydrophilic part containing hydroxyl functional groups were exposed. When TEOS was added in the alkaline condition, the exchange of the hydroxyl groups of the Igepal CO-520 with the ethyl groups of TEOS leads to the successive condensation of many TEOS molecules giving a homogenous layer of silicon dioxide on the surface of the nanoparticles. The formation of the uniform silica layer above the surface of the nanoparticles was confirmed by TEM analyses. Due to the difference in the density and refractive index of the silica and $NaYF_4$:Yb (18%), Tm (2%), the presence of slightly light layer at the surface of the dark centre in the TEM image confirms the formation of silica layer on the surface of $NaYF_4$:Yb (18%), Tm (2%) (Fig. 2d). The overall size of the synthesized $NaYF_4$:Yb (18%), Tm (2%)@SiO_2 was found by the statistical evaluation of hundred particles. The average size of the nanoparticles was found in the range of 60-65 nm as seen from particle distribution (Fig. 2e). The thickness of the silica shell is in the range of 20-30 nm.

The photoluminescence spectral analyses of the synthesized UCNPs were performed upon 980 nm

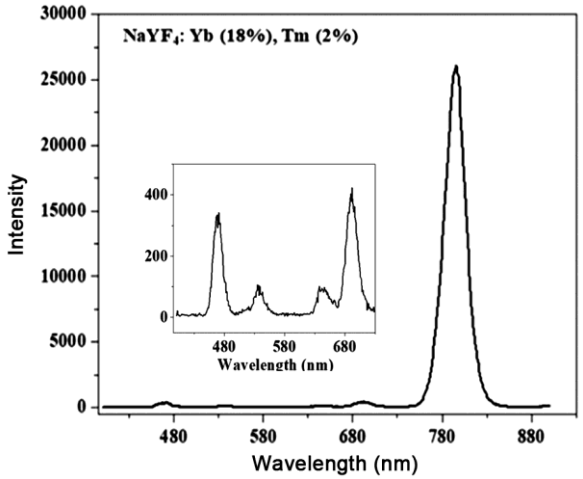

Fig. 3 — Emission spectrum of UCNPs upon 980 nm excitation

NIR excitation. The emission spectra of $NaYF_4$: 18%Yb, 2% Tm consists of blue emission bands at 450.5 and 475 nm which are attributed to the $^1O_2 \rightarrow {}^3F_4$ and $^1G_4 \rightarrow {}^3H_6$ transitions of Tm^{3+} (Fig. 3), respectively. A strong predominant NIR emission at 801.5 nm is attributed to the $^3H_4 \rightarrow {}^3H_6$ transition. Emission spectrum of $NaYF_4$: Yb (18%), Tm (2%) upon 980 nm excitation consists of peaks at 451 nm, 481 nm, 646 nm and 800 nm (Fig. 3). The dopant Yb^{3+} acts as the sensitizer due to its larger cross-section at 980 nm and transfers its energy to the co-dopant Tm^{3+} which has ladder-like energy levels. The emission at 451 nm, 481 nm, 646 nm and 800 nm, respectively, are arising due to the transitions $^1D_2 \rightarrow {}^3F_4$, $^1G_4 \rightarrow {}^3H_6$, $^1G_4 \rightarrow {}^3F_4$ and $^3H_4 \rightarrow {}^3H_6$ (Fig. 3)[29]. The decay patterns observed at 475 and 808 nm emissions during lifetime measurements (lifetime 477 and 688 μs, respectively) after exciting the UCNPs by 980 nm have been shown in Fig. 4a and Fig. 4b.

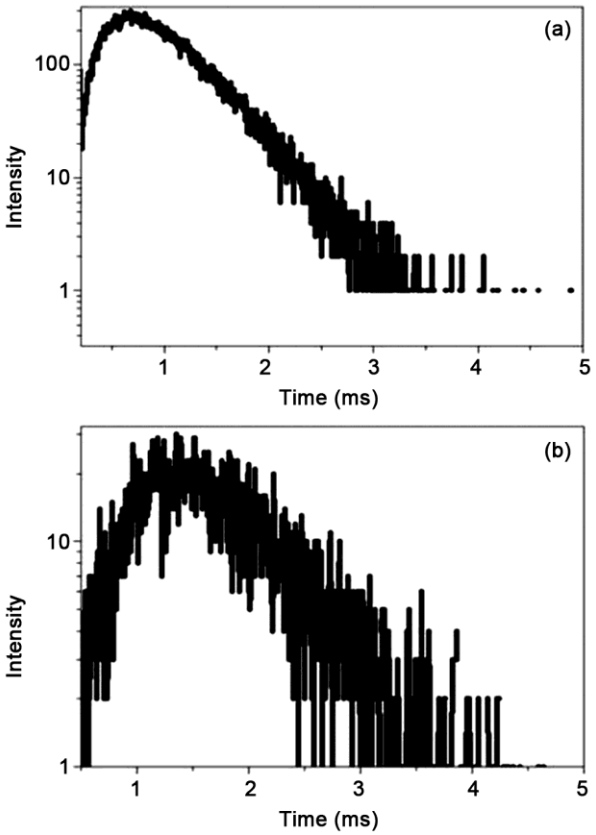

Fig. 4 — Decay of UCNPs upon 980 nm excitation at (a) wavelengths 475 (lifetime 477 μs) and (b) 808 nm (lifetime 688 μs)

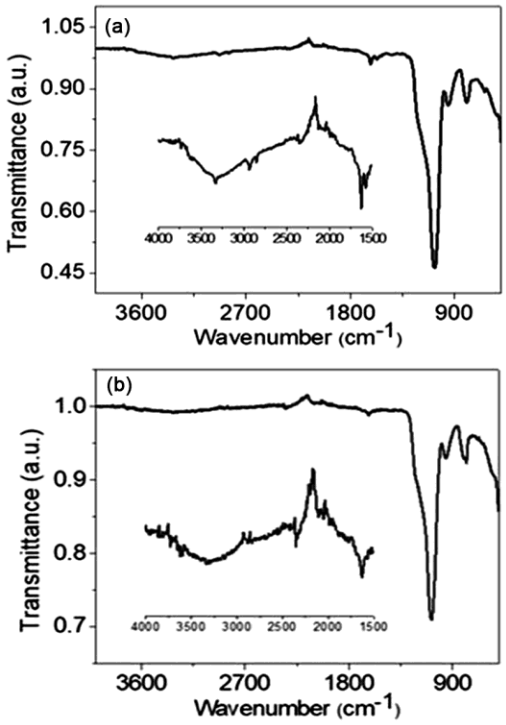

Fig. 5 — FT-IR spectra of UCNPs: $NaYF_4$: Tm, Yb@SiO_2 (a) functionalized with amine and then further (b) functionalized with 2-deoxy-D-glucose

Further, the intensity of emission of $NaYF_4$:Yb (18%), Tm (2%) under 980 nm excitation is found to depend on the power of the laser. The emission spectra were recorded upon 980 nm laser excitation with the variation of power ranging from 1.2 W to 2.4 W. The slope of the log-log plot of the intensity with the power gives the number of photons absorbed by Tm^{3+} ion to give an emission at the shorter wavelength and it was found to have value of 2. This result confirmed that the upconversion process of $NaYF_4$:Yb (18%), Tm (2%) is a two photon phenomenon[30].

For functionalization of the synthesized UCNPs, amine groups were introduced on the surface of UCNPs by treatment with APTMS. The presence of amine functional groups on the surface of UCNPs was confirmed by FT-IR spectroscopy which exhibited the broad bands centred at 1619 cm^{-1} (N-H bend) and 3360 cm^{-1} (N-H str) (Fig. 5a)[18,31-33]. The broad high-intensity band at 1061 cm^{-1} is attributable to the asymmetric stretching vibrations of bonds of Si-O-Si in SiO_2. The band at 793 cm^{-1} is due to Si-O-Si symmetric stretch, while the band at 451 cm^{-1} corresponds to the Si-O-Si or O-Si-O bending modes. The band at 964 cm^{-1} is attributable to the Si-O symmetric stretch. The band at 570 cm^{-1} is an indication of the presence of Si-O-Ln (Ln = Y^{3+}, Yb^{3+} & Tm^{3+}) (Fig. 5a)[18,31-33]. For simplicity, the obtained nanoparticles are further represented as UCNPs@SiO_2-NH_2.

The amine functional groups on the surface of UCNPs@SiO_2-NH_2 were reacted with isothiocyanate derivative of 2-deoxy-D-glucose. The reaction of amine functional groups with the isothiocynate group forming a thiourea bond is a feasible reaction even at lower temperatures. When isothiocynate derivative of 2-DG was treated with UCNPs@SiO_2-NH_2, the 2-DG moiety was attached on the surface of nanoparticles through thiourea linkage. For simplicity, the obtained nanoparticles were referred as UCNPs-2-DG. The presence of the 2-DG moieties on the surface of UCNPs-2-DG was confirmed by FT-IR spectroscopy and elemental analysis. In FT-IR spectrum, after treating amine functionalized UCNPs-NH_2 with isothiocyanate of 2-DG, the peaks at 3320 cm^{-1} for N-H str of primary amine and 2929 cm^{-1} and 2846 cm^{-1} of C-H str was suppressed by broad peak of O-H str

centred at 3248 cm^{-1} (Fig. 5b)[18,31-33]. From the elemental analysis, the percentage of sulphur content in the fixed amount of UCNPs-2-DG was found to be 3.85% while that of UCNPs-NH_2 is 0.43%. This shows that the formation of thiourea linkage which is responsible for binding of 2-DG moieties on the surface of UCNPs-2-DG.

The loading of Pt(IV) prodrug is achieved by forming ester bond between the carboxyl group[34] of Pt(IV) prodrug with the hydroxyl groups of 2-DG on the surface of UCNPs-2-DG. The synthesized Pt(IV) prodrug was authenticated by ^{1}H and $^{13}C\{^{1}H\}$ NMR spectroscopy (Supplementary Data, Figs. S10 and S11). The presence of the broad peak at 6.47 ppm with the integration of 6 protons (H) in the ^{1}H NMR represents two ammonia groups coordinated to the Pt centre. The resonances at 2.35 ppm and 2.47 ppm respectively with the integration of 5 H and 3 H represent four CH_2 groups of succinic acid attached on the hydroxyl group of the Pt(IV) prodrug. The resonances at 174.32 and 180.05 ppm in $^{13}C\{^{1}H\}$ NMR spectrum represent the carboxyl groups and resonances at 30.30 ppm and 39.85 ppm represent the hydrocarbon portions of succinic anhydride of the Pt(IV) prodrug. Further, the carboxyl group of the Pt(IV) prodrug was activated by DCC and ester coupling was performed[34]. For simplicity, the obtained nanoparticles were referred as UCNPs-Pt(IV). The amount of the Pt(IV) prodrug incorporated on the UCNPs-2-DG was quantified with ICP-OES. It is found that the percentage of loading is 85% and the amount of the Pt(IV) loaded is 10% of the weight of the UCNPs-Pt(IV) formulation.

The stock solutions of 20 mM for Pt(IV) prodrug, UCNPs-Pt(IV), 2-DG and cisplatin were prepared in 0.9 M saline solution. The MTT assay was performed by treating MCF-7 cells with cisplatin (1 µM to 10 µM), 2-DG (1 mM to 10 mM), UCNPs-2-DG (equivalent of 10 µM of UCNPs-Pt(IV)) and UCNPs-Pt(IV) (1 µM to 10 µM) and exposing to 385 nm UV light. The percentage of cell survival for after treatment of cisplatin for 10 µM is 75% and that of the prodrug is around 60%. This shows the prodrug has more potential to kill the cells. In the case of UCNPs-Pt(IV), the percentage of cell survival is around 20%. Same experiment was conducted by exposing the cells with 980 nm laser. Around 50% survival was observed for the cells treated with NP PD 10 µM and exposed with 980 nm laser, as compared to other cells kept in the dark condition. This can be explained by more internalization of the drugs inside the cancer cells because of the presence of 2-DG moieties on the surface of UCNPs-Pt(IV) (Fig. 6).

The proliferation capacities of MCF-7 cells after treating with Pt(IV) prodrug, UCNPs-2-DG and UCNPs-Pt(IV) with or without activation of the Pt(IV) prodrug by 385 nm UV light were evaluated. A representative image of MCF-7 colonies after treatment has been shown in Fig. 7. The plating efficiencies of the control and control exposed with 385 nm UV light are found to have same value of 47%. The plating efficiency of UCNPs-2-DG was found to be 38%. Taking the corresponding plating efficiencies, the survival fractions were calculated and plotted with the respective concentrations as shown in Fig. 8a and Fig. 8b

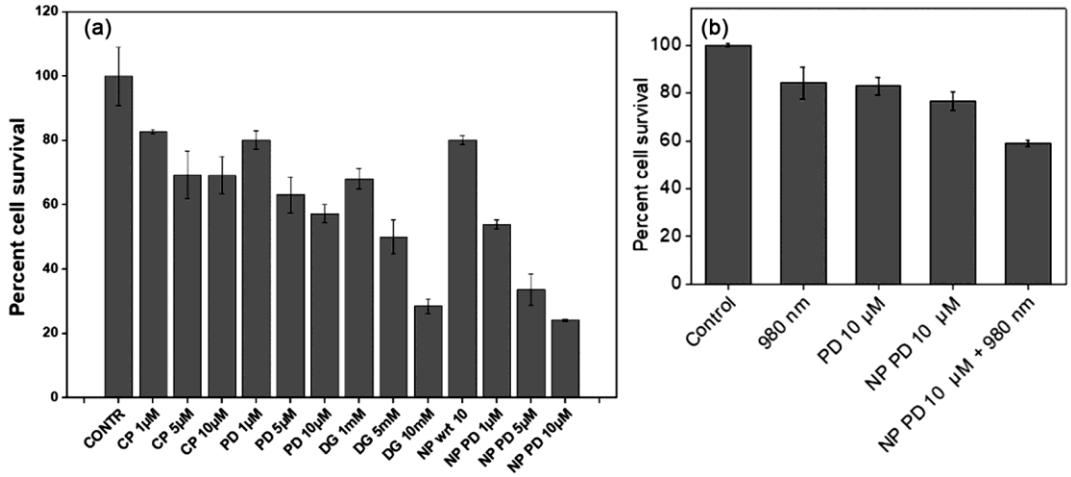

Fig. 6 — Cytotoxicity studies of Pt(IV) prodrug and Pt(IV) prodrug loaded on (a) UCNPs under light exposure and (b) 980 laser exposure conditions

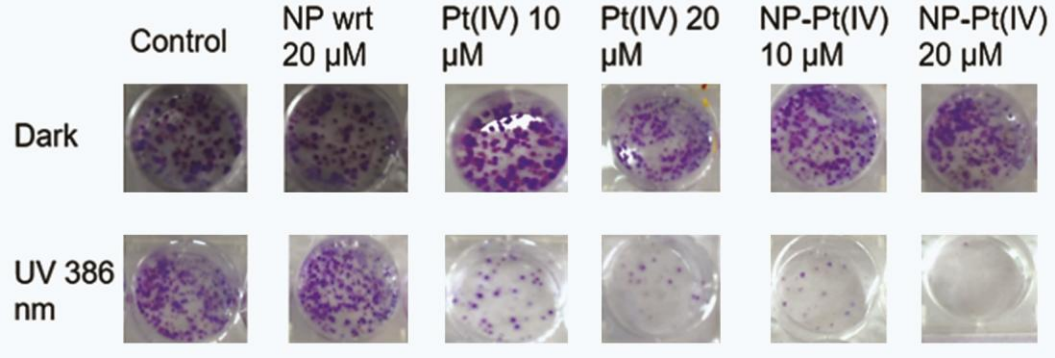

Fig. 7 — Cell proliferation assay of Pt(IV) prodrug and Pt(IV) loaded on UCNPs under dark and light exposure conditions

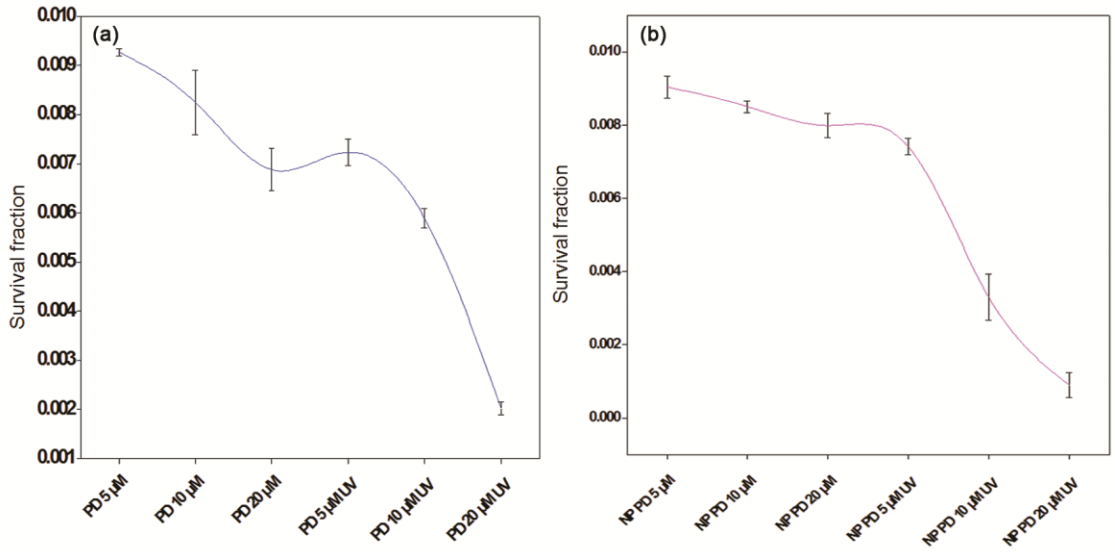

Fig. 8 — Plot of survival fractions with the respective (a) concentrations of the Pt(IV) prodrug; and (b) for formulation UCNP-Pt(IV)

Conclusion

We have synthesized the photoactivable cis-$[PtI_2(NH_3)_2(OCOCH_2CH_2COOH)_2]$, a Pt(IV) prodrug. It was loaded on nano-formulation based on $NaYF_4$:Tm, Yb upconversion nanoparticles through the conjugation with 2-deoxy-D-glucose already coated on UCNPs. Then cytotoxicity of the formulation (i) in absence of light and (ii) after exposing to 385 nm UV light was evaluated against MCF-7 cell lines by MTT assay. It revealed the enhanced cytotoxicity of UV exposed nano-formulation. The decreased surviving fraction (SF), merely 20% for UV activated formulation as compared to unexposed formulation as well as merely Pt(IV) prodrug was observed from clonogenic assay. It is a result of better internalization of a formulation within cancer cells conferred due to 2-deoxy-D-glucose rendering better efficiency to kill cancer cells. Hence it can be concluded that this photoactivable Pt(IV) loaded upconversion nanoparticles formulation is worthy for future clinical applications in cancer treatment.

Supplementary Data

Supplementary data associated with this article are available in the electronic form at http://nopr.niscair.res.in/jinfo/ijc/IJC_61(01)21-30_SupplData.pdf.

Acknowledgements

Authors are thankful to Dr. A. K. Tyagi, Director, Chemistry Group and Head, Chemistry Division, BARC, Trombay, Mumbai for the encouragement and support for this research work. Authors also acknowledge the fruitful discussions with Dr. Dibakar Goswami, Bio-Organic Division, BARC. We are thankful to Ms. Binita Kislay Kumar and Mr. Deepak V. Kathole for technical assistance during conducting biological experiments. KSS is grateful to University

Grants Commission (UGC), New Delhi for the award of fellowship.

Reference

1 (a) Wong E & Giandomenico C M, *Chem Rev*, 99 (1999) 2451; (b) Dasari S & Tchounwou P B, *Eur J Pharmacol*, 5 (2014) 364.

2 (a) Jamieson E R & Lippard S J, *Chem Rev*, 99 (1999) 2467; (b) Reedijk J, *Chem Rev*, 99 (1999) 2499.

3 (a) Siddik Z H, *Oncogene*, 22 (2003) 7265; (b) Cepeda V, Fuertes M A, Castilla J, Alonso C, Quevedo C & Pérez J M, *Anti-Can Agents Med Chem*, 7 (2007) 3.

4 (a) Oun R, Moussa Y E & Wheate N J, *Dalton Trans*, 47 (2018) 6645; (b) Florea A-M, & Büsselberg D, *Cancers*, 3 (2011) 1351.

5 (a) Johnstone T C, Suntharalingam K & Lippard S J, *Chem Rev*, 116 (2016) 3436; (b) Li X, Liu Y & Tian H, *Bioinorg Chem Appl*, 2018 (2018) Article ID 8276139.

6 (a) Tian H, Dong J, Chi X, Xu L, Shi H & Shi T, *Int J Chem Kinet*, 49 (2017) 681; (b) Wang Z, Deng Z & Zhu G, *Dalton Trans*, 48 (2019) 2536.

7 (a) Canil G, Braccini S, Marzo T, Marchetti L, Pratesi A, Biver T, Funaioli T, Chiellini F, Hoeschele J D & Gabbiani C, *Dalton Trans*, 48 (2019) 10933; (b) Shi H, Romero-Canelón I, Hreusova M, Novakova O, Venkatesh V, Habtemariam A, Clarkson G J, Song J-i, Brabec V & Sadler P J, *Inorg Chem*, 57 (2018) 14409; (c) Gandioso A, Shaili E, Massaguer A, Artigas G, González-Cantó A, Woods J A, Sadler P J & Marchán V, *Chem Commun*, 51 (2015) 9169; (d) Bednarski P J, Mackay F S & Sadler P J, *Antican Agents Med Chem*, 7 (2007) 75; (e) Mackay F S, Woods J A, Heringová P, Kašpárková J, Pizarro A M, Moggach S A, Parsons S, Brabec V & Sadler P J. *PNAS*, 104 (2007) 20743.

8 Shi H, Imberti C & Sadler P J, *Inorg Chem Front*, 6 (2019) 1623.

9 Thiabaud G, McCall R, He G, Arambula J F, Siddik Z H & Sessler L, *Angew Chem Int Ed Engl*, 55 (2016) 12626.

10 (a) Perfahl S, Natile M M, Mohamad H S, Helm C A, Schulzke, C, Natile G & Bednarski P J, *Mol Pharmaceutics*, 13 (2016) 2346; (b) Wu X, Chen G, Shen J, Li Z, Zhang Y & Han G, *Bioconjug Chem*, 26 (2015) 166; (c) Qiu H, Tan M, Ohulchanskyy T Y, Lovell J F & Chen G, *Nanomater*, 8 (2018) Article ID 344.

11 Zhu X, Su Q, Feng W & Li F, *Chem Soc Rev*, 46 (2017) 1025.

12 (a) Rafique R, Baek S H, Park C Y, Chang S J, Gul A R, Ha S, Nguyen T P, Oh H, Ham S, Arshad M, Lee H & Park T J, *Sci Rep*, 8 (2018) Article ID 17101; (b) Lee G & Park Y Il, *Nanomater*, 8 (2018) Article ID 511; (c) Bagheri A, Arandiyan H, Boyer C & Lim M, *Adv Sci*, 3 (2016) Article ID 1500437.

13 (a) Dong H, Du S-R, Zheng X-Y, Lyu G-M, Sun L-D, Li L-D, Zhang P-Z, Zhang C & Yan C-H, *Chem Rev*, 115 (2015) 10725; (b) Chen G, Qiu H, Prasad P N & Chen X, *Chem Rev*, 114 (2014) 5161; (c) Wang C, Cheng L & Liu Z, *Theranostics*, 3 (2013) 317; (d) Chen Q, Chen Q, Chen F & Zhang Q, *J Mater Chem*, 21 (2011) 7661; (e) Kazi J, Mukhopadhyay R, Sen R, Jha T, Ganguly S M & Chatterjee D, *Chem Commun*, 10 (2019) 559.

14 (a) Li S D & Huang L, *Biochim Biophys Acta*, 1788 (2009) 2259; (b) Uster P S, Allen T M, Daniel B E, Mendez C J, Newman M S & Zhu G Z, *FEBS Lett*, 386 (1996) 243.

15 Gaur U, Sahoo S K, De T K, Ghosh P C, Maitra A & Ghosh P K, *Int J Pharmac*, 202 (2000) 1.

16 (a) Warburg O, Wind F & Negelein E, *J Gen Physiol*, 8 (1927) 519; Pavlova1 N N & Thompson C B, *Cell Metabol*, 12 (2016) 1; (b) Koppenol W H, Bounds P L & Dang C V, *Nat Rev Can*, 11 (2011) 325.

17 Ralser M, Wamelink M M, Struys E A, Joppich C, Krobitsch S, Jakobs C & Lehrach H A, *PNAS*, 105 (2008) 17807.

18 Sharma K S, Dubey A K, Koijam A S, Kumar C, Ballal A, Mukherjee S, Phadnis P P & Vatsa R K, *New J Chem*, 44 (2020) 13834.

19 Armarego W L F & Perrin D D, *Purification of Laboratory Chemicals (4th Edn)*. (Pergamon, Oxford) 1996.

20 (a) Chen X, Zhao Z, Jiang M, Que D, Shia S & Zheng N, *New J Chem*, 37 (2013) 1782; (b) Mallqui C R, Puga R, Acosta D, Hernandez J M & Loro H, *New J Chem*, 37 (2013) 1782.

21 Liu J-N, Bu W-B & Shi J-L, *Acc Chem Res*, 48 (2015) 1797.

22 (a) Shi Y, Liu S-A, Kerwood D J, Goodisman J & Dabrowiak J C, *J Inorg Biochem*, 107 (2012) 6; (b) Dhara S C, *Ind J Chem*, 8 (1970) 193; (c) Alderden R A, Hall M D & Hambley T W, *J Chem Educ*, 83 (2006) 728.

23 Hermanson G T, *Bioconjugate Techniques*, (Academic Press, London) 1996.

24 Mossman T, *J Immunol Methods*, 65 (1983) 55.

25 Maikho T, Patwardhan R S, Das T N, Sharma D & Sandur S K, *Free Radic Res*, 52 (2018) 212.

26 Franken N A P, Rodermond H M, Stap J, Haveman J & Bree C V, *Nat Protocols*, 1 (2006) 2315.

27 (a) Sedlmeier A & Gorris H H, *Chem Soc Rev*, 44 (2015) 1526; (b) Muhr V, Wilhelm S, Hirsch T, Wolfbeis O S, *Acc Chem Res*, 47 (2014) 3481.

28 Manurung R V, Wirant G and Hermida I D P, *IOP Conf Ser Mater Sci Eng*, 367 (2018) 012043.

29 Yi G-S & Chow G-M, *Chem Mater*, 19 (2007) 341.

30 Auzel F, *Chem Rev*, 104 (2004) 139.

31 Shafqat S S, Khan A A, Zafar M N, Alhaji M H, Sanaullah K, Shafqat S R, Murtaza S & Pang S C, *J Mater Res Technol*, 8 (2019) 385.

32 Jung H-S, Moon D-S & Lee J-K, *J Nanomater*, 2012 (2012) Article ID 593471.

33 Guodong F, Mingming G, Qi L, Hongyu M, Guanghua L, Qiang M, Qiang F, Yanfu H & Zhiguang S, *New J Chem*, 40 (2016) 8444.

34 Neises B & Steglich W, *Angew Chem Int Ed*, 17 (1978) 522.